Light fidelity for interference-free communication of critical medical devices

Quantifying electromagnetic immunity margins, link budget and latency bounds for an intensive-care bay

[1]Pravat Satpathy, [2] Sonia Mohapatra
[1]Researcher, [2]Researcher,
[1,2] R & D Division
[1,2]Tekstein Solutions, India
[1]pravat@teksteinsolutions.com , sonia@teksteinsolutions.com

Abstract—Critical-care devices exchange waveform and alarm data continuously, yet the radio spectrum around a bed is both congested and, from the standpoint of device immunity, hostile: the same transmitters that carry the traffic are the disturbance the equipment must survive. This paper states the coupling mechanism quantitatively against IEC 60601-1-2, then develops and evaluates a light fidelity (LiFi) replacement for the last hop. A closed-form chain covering the Lambertian channel, shot- and thermal-noise-limited signal-to-noise ratio, error probability for on-off keying and M-ary quadrature amplitude modulation on a direct-current-biased optical multicarrier waveform, delay spread, deterministic access latency and diversity outage is applied to a 7 m square intensive-care bay served by four ceiling luminaires. The link yields 53.4 to 313.4 μW of received power, 40.2 to 55.4 dB of signal-to-noise ratio, a worst-case margin of 24.6 dB over the 15.6 dB needed for a bit error ratio of 10^{-9}, complete coverage at that error ratio and a uniform 100 Mbit/s payload rate while sustaining 233 lux. Delay spread stays below 4.4 ns so no equaliser is required at 20 MHz. Worst-case delivery latency is bounded at 0.595 ms against 13.08 ms for a contended radio baseline, and four-fold access-point diversity gives 6.3×10^{-6} outage. A 200 mW radio client is shown to exceed the 3 V/m general immunity level within 0.82 m and to induce about 318 mV on an unshielded lead at 0.3 m, roughly 50 dB above the biopotential of interest, whereas the optical front end contains no intentional radiator. *(Abstract)*

Index Terms—Light fidelity, visible light communication, electromagnetic interference, medical device safety, IEC 60601-1-2, intensive care, latency bound. *(key words)*

I. Introduction

An occupied intensive-care bay may host a multi-parameter monitor streaming electrocardiogram and plethysmography waveforms, a ventilator reporting pressure and flow curves hundreds of times a second, several smart infusion pumps, a dialysis machine and a barcode scanner, all of which are expected to reach the clinical information system and the alarm distribution service. The prevailing answer has been radio, and it produces a compound problem. The unlicensed bands are contended, so the delay of an alarm packet is a heavy-tailed random variable rather than a bounded quantity; and the transmitters producing that contention sit centimetres from equipment certified at a modest immunity field strength, so the network is also the disturbance.

Both symptoms share one cause: an omnidirectional, wall-penetrating carrier used inside a space where confinement is desirable. Light fidelity (LiFi) modulates the intensity of a solid-state luminaire and detects it with a photodiode [3], [5]. It is not another band but a carrier stopped by the same opaque surfaces that define a clinical space, and generated without an intentional radiator in the sense of the immunity standards. This paper contributes a quantitative statement of the interference mechanism, a complete analytical design chain for an optical bedside link, and a numerical evaluation reporting margins against thresholds a clinical engineering department would be asked to accept.

II. The Interference Problem

Interference in a hospital seldom appears as loss of function. It appears as an implausible heart rate, a spurious occlusion alarm, an inhibited pacing beat or a misreported tidal volume. Investigations of mobile handsets in critical care have reported incidents across a substantial fraction of tested devices, including infusion stoppage and misreading of physiological parameters [1]; the resulting alarm burden recurs in published inventories of health-technology hazards [20]. Three properties make the setting vulnerable: proximity, since a clinician holds a handset at the bedside rail; signal level, since a surface electrocardiogram is of the order of 1 mV; and the transfer path, since patient leads are long, deliberately unshielded and terminate in high-impedance amplifiers, which approximates a receiving antenna followed by an envelope detector once junction non-linearity is admitted.

IEC 60601-1-2 sets the radiated immunity levels equipment must withstand while retaining essential performance [2]: broadly 3 V/m over the general sweep and of the order of 10 V/m at the mobile-service spot frequencies for equipment used close to portable transmitters. For a transmitter radiating P_t into a gain G, the far-field strength at separation d is Eq. 1; inverting it gives the radius inside which a limit E_{lim} is violated, which is the only quantity an installation can actually enforce.

$$E = \sqrt{(30\, P_t G)} / d\,, \quad d_{min} = \sqrt{(30\, P_t G)} / E_{lim} \tag{1}$$

The field does not damage the instrument; the differential voltage it induces does. Treating an unshielded lead pair as a resonant structure of effective length $l_{eff} \approx \lambda/\pi = c/(\pi f)$, the open-circuit voltage at the front end is Eq. 2.

$$V_{oc} = E \cdot l_{eff} = Ec / (\pi f) \quad (2)$$

At 2.45 GHz the effective length is 39.0 mm, so a 200 mW client at 0.3 m presents about 318 mV to an amplifier resolving 1 mV of biopotential, a ratio near 50 dB. The carrier lies outside the diagnostic passband and is largely rejected, but the burst structure of a packet radio modulates it at kilohertz rates and any junction non-linearity rectifies that envelope straight into the measurement band. Table 1 evaluates Eq. 1 and Eq. 2 for bedside transmitter classes; the final column is the radius inside which 3 V/m is exceeded. For a legacy handset it exceeds the whole bay.

Table 1 Incident field and induced lead voltage for bedside radio sources

Radio source	E at 0.1 m (V/m)	E at 0.3 m (V/m)	E at 1.0 m (V/m)	Voc at 0.3 m (mV)	Radius for E > 3 V/m (m)
Handset, 2 W (legacy cellular)	77.5	25.8	7.75	1006	2.58
RFID reader, 1 W, G = 1.64	70.1	23.4	7.01	911	2.34
WLAN client, 200 mW	24.5	8.16	2.45	318	0.82
WLAN access point, 100 mW	17.3	5.77	1.73	225	0.58
Bluetooth low energy tag, 2.5 mW	2.74	0.91	0.27	36	0.09
Proposed LiFi optical front end	nil	nil	nil	nil	not applicable

The temporal half of the problem follows from contention. A station that senses the medium busy defers, draws a random backoff and doubles its window after each failure, so with a dozen contenders and a packet error ratio inflated by the interference above, the delay distribution acquires a long tail. Because the carrier passes through plasterboard, the neighbouring bay and the corridor share the collision domain, so the offered load cannot be bounded at design time. The conventional remedies — separation distance, band migration, shielding, administrative bans — are all partial, because none of them alters the fact that the chosen carrier propagates freely into a volume where it is unwelcome. Changing the carrier does.

III. System Model

A. Optical channel

Following the established indoor formulation [4], [10], a phosphor-converted luminaire is a generalised Lambertian source of mode number $m = -\ln 2 / \ln(\cos \varphi_{½})$. The line-of-sight gain to a photodiode of area A_r at distance d, irradiance angle φ and incidence angle ψ is Eq. 3, with filter transmittance T_s and non-imaging concentrator gain $g(\psi) = n^2/\sin^2\Psi_c$ inside the field of view Ψ_c.

$$H(0) = [(m+1)A_r / 2\pi d^2] \cos m(\varphi)\ T_s g(\psi) \cos(\psi), \quad 0 \le \psi \le \Psi_c \quad (3)$$

Total received power sums the K co-visible luminaires and the first-order wall term, Eq. 4, in which each wall patch of area dA and reflectance ρ re-emits Lambertian towards the receiver.

$$P_r = \Sigma_k H_k(0) P_{t,k} + \Sigma_{walls} [(m+1)A_r \rho\ dA / 2\pi^2 d_1^2 d_2^2] \cos m\theta \cos\theta_{in} \cos\theta_{out} \cos\psi\ T_s g(\psi)\ P_t \quad (4)$$

B. Noise and signal-to-noise ratio

With responsivity R and modulation index ξ the signal photocurrent is $\xi R P_r$. Shot noise arises from the signal and, dominantly indoors, from the ambient photocurrent I_{bg}; front-end thermal noise follows the two-term field-effect-transistor model [4], [10]. Eq. 5 and Eq. 6 give the two variances and Eq. 7 the electrical signal-to-noise ratio, where q is the electronic charge, B the noise bandwidth, T_K absolute temperature, G_{ol} the open-loop gain, C_{pd} the photodiode capacitance per unit area, Γ the channel noise factor, g_m the transconductance and I_2, I_3 the noise-bandwidth factors.

$$\sigma^2_{shot} = 2qRP_rB + 2qI_{bg}I_2B \quad (5)$$

$$\sigma^2_{th} = (8\pi k T_K/G_{ol}) C_{pd} A_r I_2 B^2 + (16\pi^2 k T_K \Gamma / g_m) C_{pd}^2 A_r^2 I_3 B^3 \quad (6)$$

$$\text{SNR} = (\xi R P_r)^2 / (\sigma^2_{shot} + \sigma^2_{th}) \quad (7)$$

C. Error probability, margin and rate

Error probability for on-off keying and for the M-ary quadrature amplitude constellations of a direct-current-biased optical multicarrier waveform are Eq. 8 and Eq. 9 [8], [9]. Inverting Eq. 8 at a target of 10^{-9} requires 15.56 dB, so the design margin at any point is Eq. 10. Hermitian symmetry halves the usable bandwidth, giving Eq. 11 for adaptive loading with a 3 dB implementation penalty. For a safety-related link the margin, not the rate, is the meaningful figure of merit.

$$\text{BER}_{OOK} = Q(\sqrt{\text{SNR}}) \quad (8)$$

$$\text{BER}_{M\text{-}QAM} = [4/\log_2 M](1 - 1/\sqrt{M}) Q(\sqrt{[3 \log_2 M \cdot \text{SNR} / (M-1)]}) \quad (9)$$

$$\Delta_{dB} = 10 \log_{10}\text{SNR} - 10 \log_{10}\text{SNR}_{req} \quad (10)$$

$$R_b = (B/2) \log_2 M, \quad M = \max\{M : \text{SNR}_{dB} \ge \text{SNR}_{req}(M) + 3\} \quad (11)$$

D. Dispersion, latency and diversity

From the power–delay profile $\{P_i, \tau_i\}$ of the line-of-sight and first-order terms, the root-mean-square delay spread is Eq. 12 with mean delay $\mu_\tau = \Sigma P_i \tau_i / \Sigma P_i$, and the coherence bandwidth is $B_c \approx 1/(10 D_{rms})$. Holding the modulation bandwidth below B_c keeps the channel flat and removes the equaliser and its latency.

$$D_{rms} = \sqrt{[\ \Sigma P_i(\tau_i - \mu_\tau)^2 / \Sigma P_i\ ]} \quad (12)$$

Access uses a superframe T_{sf} in which every life-support device owns a guaranteed slot, so delivery latency is Eq. 13 and its deterministic bound over $n_{r,max}$ retries is Eq. 14, the retry count being governed by the packet error ratio $1 - (1 - \text{BER})^L$. Finally, if a device sees N_{AP} access points each independently obstructed with probability p_b, outage requires simultaneous blockage of all paths, Eq. 15.

$$T_d = U(0,T_{sf}) + n_r T_{sf} + L/R_b + T_p \quad (13)$$
$$T_{d,max} = (1 + n_{r,max})T_{sf} + L/R_b + T_p \quad (14)$$
$$P_{out} = p_b{}^{\wedge}N_{AP}, \quad A_{link} = 1 - p_b{}^{\wedge}N_{AP} \quad (15)$$

IV. Proposed Architecture and Simulation Setup

Fig. 1 replaces the general lighting of one bay with four modulation-capable luminaires on a square grid, each fed by power over Ethernet from a bay-level edge gateway. The downlink is visible; the uplink uses a few milliwatt of near-infrared aimed at the ceiling so that no visible flicker is added at the patient. Each device carries a silicon photodiode of 1 cm^2 with a hemispherical concentrator, a blue-pass filter rejecting the slow phosphor component, a transimpedance amplifier and a fixed-function modem, and deliberately no radio, so a device fitted with the module introduces no new emission into the bay.

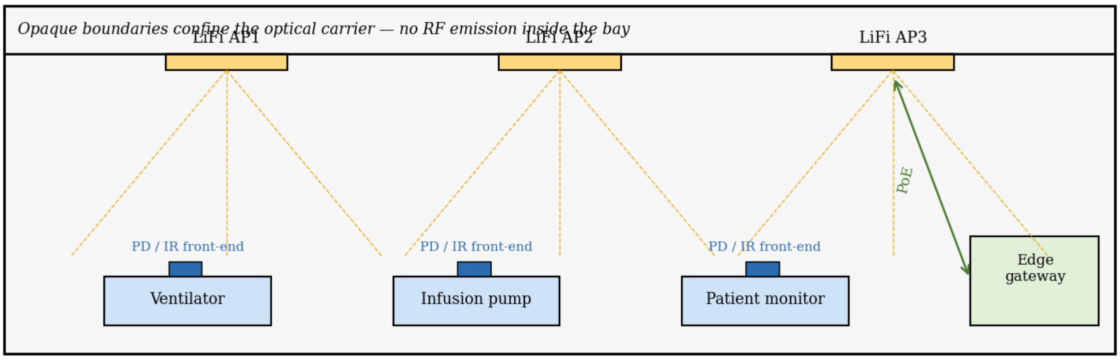

Fig. 1 Proposed bay-level architecture. Four modulation-capable luminaires form overlapping optical cells; devices carry a photodiode receiver and an infrared uplink; the edge gateway aggregates traffic over a wired backhaul.

The medium-access layer runs a 500 µs superframe: a beacon, a contention-free region holding one guaranteed slot per life-support device, then a short contention region for non-critical traffic. Because the cell is bounded by the walls, the population of the contention-free region is known at commissioning and Eq. 14 is a design constant rather than an estimate. Devices are quasi-static, so overlapping cells are combined at the receiver rather than handed over. Graceful degradation is explicit: after three lost superframes the device asserts a local annunciator and falls back to the wired nurse-call bus, and no safety function is permitted to depend on the wireless link.

Eq. 1 to Eq. 15 were evaluated over a 7 × 7 × 3 m bay with the receiver plane at 1 m, on a 141 × 141 grid of 5 cm resolution. Delay spread was computed at three positions by summing the line-of-sight terms with 1600 first-order patches per wall per luminaire at ρ = 0.7. Latency was obtained by Monte Carlo over 3×10^5 packets for the guaranteed-slot scheme and for a distributed-coordination baseline with twelve contenders, a 9 µs slot, a 34 µs interframe space, binary exponential backoff from a window of sixteen and an 8 % packet error ratio representative of a congested band. Robustness was assessed by sweeping ambient photocurrent from one to fifty times nominal and by applying up to 30 dB of extra loss for soiling, ageing and partial shadowing. Table 2 lists the parameters.

Table 2 Simulation parameters

Parameter	Value	Parameter	Value
Bay, receiver plane	7 × 7 × 3 m, h = 1.0 m	Modulation bandwidth B	20 MHz
Access points	4, at ±1.75 m from centre	Modulation index ξ	0.5
Optical power per AP	15 W	Ambient photocurrent Ibg	5100 µA nominal
Semi-angle φ½ (mode m)	60° (m = 1.00)	Noise factors I2 / I3	0.562 / 0.0868
Photodiode area Ar	1.0 cm^2	Gol / Cpd	10 / 112 pF·cm^{-2}
Responsivity R	0.53 A/W	Γ / gm	1.5 / 30 mS
Field of view Ψc	70°	Wall reflectance ρ	0.7
Concentrator n / g(ψ)	1.5 / 2.55	Superframe Tsf, payload L	500 µs, 200 byte
Filter transmittance Ts	0.90	Luminous efficacy	250 lm/W optical

V. Results and Discussion

A. Link budget, coverage and rate

The grid produces 233 lux mean horizontal illuminance over the central 6 × 6 m area with a 114 lux minimum and 0.49 uniformity, consistent with EN 12464-1 patient-room levels outside procedure periods [19], so the communication function does not compromise the primary purpose of the fitting. Received power, Fig. 2(a), spans 53.4 to 313.4 µW with a mean of 187.6 µW, its minima at the corners where the irradiance angle to every luminaire is large.

Evaluating Eq. 5 to Eq. 7 shows the link is comprehensively shot-noise limited: the ambient term contributes 1.84×10^{-14} A^2 against 5.43×10^{-16} A^2 of thermal noise, so front-end design accounts for only 2.9 % of total noise power and performance is governed by the optical budget and ambient light control. Signal-to-noise ratio, Fig. 2(b), ranges from 40.2 dB at the extreme corner to 55.4 dB beneath a luminaire, mean 50.5 dB, fifth percentile 45.4 dB; restricting attention to the working area more than 0.5 m from the walls raises the worst case to 45.9 dB. Fig. 2(c) shows that 100 % of the bay clears the 15.56 dB threshold by at least 24.6 dB, with a mean margin of 35.0 dB.

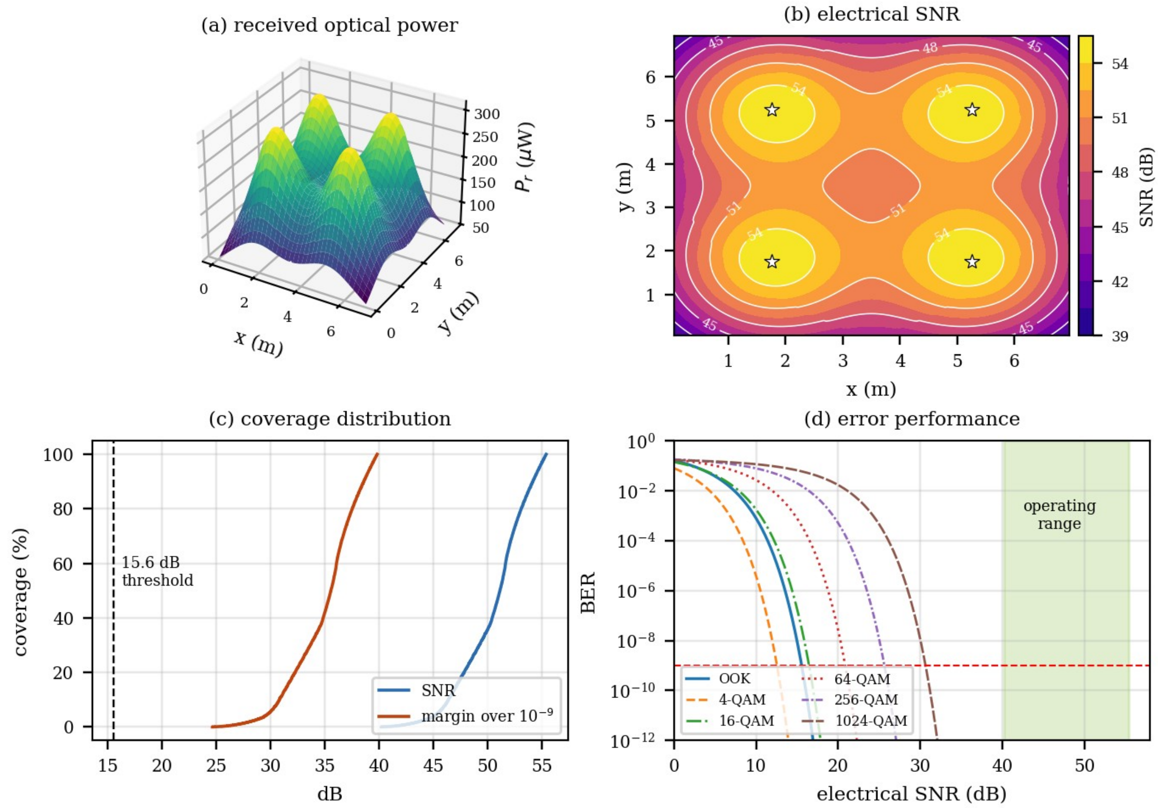

Fig. 2 Simulated link performance. (a) received optical power on the device plane; (b) electrical signal-to-noise ratio, stars marking luminaires; (c) cumulative coverage of signal-to-noise ratio and of margin over the 10^{-9} threshold; (d) error probability with the simulated operating range shaded.

Fig. 2(d) places that operating range on the curves of Eq. 8 and Eq. 9. The whole coverage area lies to the right of every constellation threshold considered, from 12.5 dB for quaternary to 30.7 dB for the 1024-point constellation, so adaptive loading under Eq. 11 selects the highest order everywhere and the bay delivers a uniform 100 Mbit/s per cell, 400 Mbit/s aggregate, with complete coverage at 10^{-9}. The link is therefore bandwidth-limited rather than power-limited, in contrast with laboratory demonstrations that spend every decibel on record aggregate rates [14]; the surplus of some 25 dB is available as margin instead. Against demand this is ample: a fully instrumented bed generating a twelve-lead electrocardiogram at 96 kbit/s, ventilator waveforms at 30 kbit/s, capnography and oximetry at 8 kbit/s and pump and alarm messaging at 3 kbit/s needs 137 kbit/s, so even at 60 % access efficiency one cell supports over four hundred such device sets. Root-mean-square delay spread from Eq. 12 is 1.41 ns at the centre, 2.66 ns at a bedside position and 4.37 ns in a corner, giving coherence bandwidths of 71.1, 37.5 and 22.9 MHz; the 20 MHz operating point stays below all three, so the channel is flat and no equaliser is needed. The corner value is the binding constraint on any future rate increase.

B. Electromagnetic compatibility and latency

Fig. 3(a) plots Eq. 1 against the immunity levels of IEC 60601-1-2. The 3 V/m general level is exceeded within 0.58 m of a 100 mW access point, 0.82 m of a 200 mW client and 2.58 m of a 2 W handset; the 10 V/m life-support level is exceeded within 0.17, 0.24 and 0.77 m respectively. Where a clinician stands at the rail and a tablet rests on the ventilator trolley these radii are routinely violated in normal use. The optical alternative has no equivalent curve: the transmitter is a light-emitting diode driven at a few tens of megahertz behind a metal housing, so the only radio-frequency emission is unintentional driver noise bounded by CISPR 11 [18] and orders of magnitude below the immunity floor at a neighbouring enclosure. The disturbance is removed from the bay rather than reduced, which is qualitatively different from any separation-distance policy.

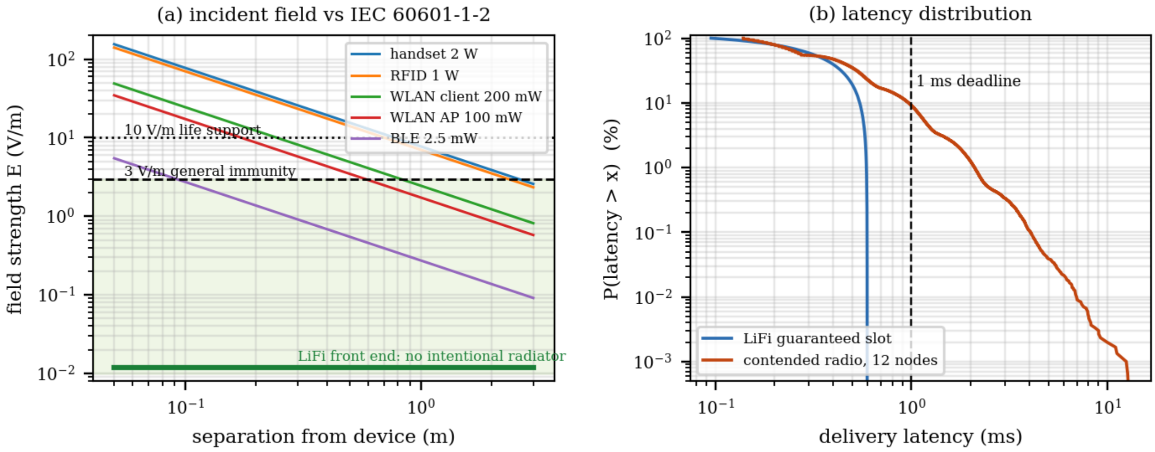

Fig. 3 Compatibility and timing. (a) incident field strength against separation for bedside radio sources, compared with IEC 60601-1-2 immunity levels; (b) complementary cumulative distribution of delivery latency for the guaranteed-slot optical link and a contended radio baseline.

Fig. 3(b) and Table 3 compare delivery latency. The comparison is instructive because the optical scheme is not uniformly faster: its 0.345 ms mean is of the same order as the 0.481 ms of the baseline and its 0.346 ms median is slightly worse than 0.376 ms, since a slotted scheme always pays half a superframe of access delay. The difference is in the tail. The optical scheme is bounded at 0.595 ms with a jitter of 0.50 ms, which is simply the superframe, while the baseline reaches 2.10 ms at the ninety-ninth percentile, 6.97 ms at the ninety-nine point nine nine percentile and 13.08 ms worst observed, a jitter of 6.83 ms. For a safety-related alarm the requirement is a deadline, not an average: against 1 ms the optical scheme complies by construction whereas the baseline misses roughly one packet in a hundred.

Table 3 Delivery latency for a 200-byte alarm payload

Scheme	Mean (ms)	99th pct (ms)	99.99th pct (ms)	Worst observed (ms)
Proposed LiFi, guaranteed slot	0.345	0.590	0.595	0.595
Contended radio, 12 contenders	0.481	2.102	6.970	13.084
Improvement factor	0.72×	3.6×	11.7×	22.0×

C. Robustness and availability

Fig. 4(a) applies Eq. 15. At a five percent per-path blockage probability one access point yields 5×10^{-2} unavailability, two 2.5×10^{-3}, three 1.25×10^{-4} and four 6.25×10^{-6}, so the four-luminaire grid crosses a 10^{-5} target with margin; even at a pessimistic twenty percent it reaches 1.6×10^{-3}, which the wired fallback covers. Fig. 4(b) sweeps the ambient photocurrent of Eq. 5: a fiftyfold increase, a severe representation of an examination luminaire directly overhead, reduces the worst-case signal-to-noise ratio from 40.2 to 23.4 dB, still 7.8 dB above the on-off-keying threshold although adaptive loading would drop the constellation order locally. Fig. 4(c) applies uniform extra loss: coverage at 10^{-9} is unaffected to 10 dB, falls to 94.7 % at 15 dB and collapses beyond 20 dB, so a maintenance policy holding cumulative soiling and ageing below 10 dB preserves full performance and 15 dB indicates service.

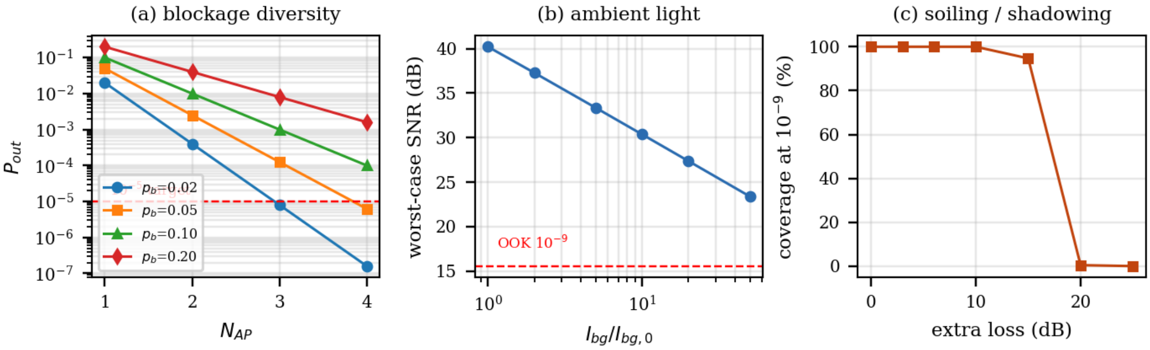

Fig. 4 Robustness. (a) outage against the number of co-visible access points for several per-path blockage probabilities; (b) worst-case signal-to-noise ratio against ambient photocurrent multiplier; (c) coverage at 10^{-9} against additional shadowing or soiling loss.

Radio retains the advantages of mobility and low retrofit cost, while light wins on interference, containment and determinism, which suggests a hybrid deployment rather than wholesale replacement: the optical link serves the fixed, safety-related devices inside the bay and a radio overlay continues to serve mobile staff terminals and asset tracking outside it. Overlapping cells also admit joint transmission and optimum combining, which would raise the corner margin further [13], [15]; such coexistence architectures have been studied in a general setting [11], [12] and map naturally onto the clinical case, where the boundary between fixed and mobile equipment is well defined.

VI. Limitations

The channel model includes line-of-sight and first-order reflections only, so the reported coherence bandwidths are mildly optimistic, though the 20 MHz operating point retains wide margin. Eq. 15 assumes independent paths, which a single large obstruction such as a mobile radiography unit violates; angular-diversity receivers and the wired fallback are the mitigations, and correlated blockage from measured occupancy traces is the natural extension. Clinically, the device-side window must survive repeated disinfection without hazing given the 10 dB soiling limit; optical output requires assessment under IEC 62471 [16] and any infrared uplink under IEC 60825-1 [17]; and night-time dimming forces either a pulse-position scheme that preserves average optical power or a shift entirely to infrared. The study is analytical and simulation-based, and bench validation with real life-support equipment, including conducted and radiated emission measurement of the luminaire driver, is required before any claim of clinical readiness.

VII. Conclusion

Bedside connectivity in critical care was framed as one problem with two symptoms — disturbance of sensitive instrumentation and an unbounded delay tail on safety-related messages — both traceable to a wall-penetrating carrier used where confinement is wanted. A 200 mW client was shown to exceed the 3 V/m general immunity level within 0.82 m and to present about 318 mV to an unshielded lead at 0.3 m, some 50 dB above the biopotential measured. An optical replacement evaluated for a 7 m square bay with four luminaires achieves 40.2 to 55.4 dB of signal-to-noise ratio, a worst-case margin of 24.6 dB over the 10^{-9} threshold, complete coverage, a uniform 100 Mbit/s against a 137 kbit/s per-bed requirement, delay spread below 4.4 ns so no equaliser is needed at 20 MHz, latency bounded at 0.595 ms against a 13.08 ms worst case for contended radio, and 6.3×10^{-6} outage with four-fold diversity, while retaining 7.8 dB of margin under a fiftyfold ambient increase and tolerating 10 dB of soiling. The margins are comfortable rather than marginal, and the surplus is best spent on robustness rather than throughput. Future work will address correlated blockage, a dimming-compatible modulation, joint transmission across cells and an instrumented bench validation.

Acknowledgment

The author thanks the engineering team at Tekstein Solutions for discussions on clinical device integration and for reviewing the interference-coupling argument of Section II.

References

[1] E. J. van Lieshout, S. N. van der Veer, R. Hensbroek, J. C. Korevaar, M. B. Vroom, and M. J. Schultz, "Interference by new-generation mobile phones on critical care medical equipment," Critical Care, vol. 11, no. 5, R98, 2007.

[2] IEC 60601-1-2, Medical electrical equipment — Part 1-2: General requirements for basic safety and essential performance — Collateral standard: Electromagnetic disturbances, 4th ed., International Electrotechnical Commission, Geneva, 2014, with Amendment 1, 2020.

[3] H. Haas, L. Yin, Y. Wang, and C. Chen, "What is LiFi?," Journal of Lightwave Technology, vol. 34, no. 6, pp. 1533–1544, March 2016.

[4] T. Komine and M. Nakagawa, "Fundamental analysis for visible-light communication system using LED lights," IEEE Transactions on Consumer Electronics, vol. 50, no. 1, pp. 100–107, February 2004.

[5] J. M. Kahn and J. R. Barry, "Wireless infrared communications," Proceedings of the IEEE, vol. 85, no. 2, pp. 265–298, February 1997.

[6] IEEE Std 802.15.7-2018, IEEE standard for local and metropolitan area networks — Part 15.7: Short-range optical wireless communications, IEEE, 2019.

[7] IEEE Std 802.11bb-2023, IEEE standard for information technology — Amendment 7: Light communications, IEEE, 2023.

[8] J. Armstrong, "OFDM for optical communications," Journal of Lightwave Technology, vol. 27, no. 3, pp. 189–204, February 2009.

[9] S. Dimitrov and H. Haas, Principles of LED Light Communications: Towards Networked Li-Fi. Cambridge, U.K.: Cambridge University Press, 2015.

[10] Z. Ghassemlooy, W. Popoola, and S. Rajbhandari, Optical Wireless Communications: System and Channel Modelling with MATLAB, 2nd ed. Boca Raton, FL: CRC Press, 2019.

[11] M. Ayyash et al., "Coexistence of WiFi and LiFi toward 5G: concepts, opportunities, and challenges," IEEE Communications Magazine, vol. 54, no. 2, pp. 64–71, February 2016.

[12] P. H. Pathak, X. Feng, P. Hu, and P. Mohapatra, "Visible light communication, networking, and sensing: a survey, potential and challenges," IEEE Communications Surveys and Tutorials, vol. 17, no. 4, pp. 2047–2077, 2015.

[13] C. Chen, D. Tsonev, and H. Haas, "Joint transmission in indoor visible light communication downlink cellular networks," in Proc. IEEE Globecom Workshops, Atlanta, GA, 2013, pp. 1127–1132.

[14] D. Tsonev, S. Videv, and H. Haas, "Towards a 100 Gb/s visible light wireless access network," Optics Express, vol. 23, no. 2, pp. 1627–1637, 2015.

[15] Y. S. Eroglu, I. Guvenc, A. Sahin, Y. Yapici, N. Pala, and M. Yuksel, "Multi-element VLC networks: LED assignment, power control, and optimum combining," IEEE Journal on Selected Areas in Communications, vol. 36, no. 1, pp. 121–135, January 2018.

[16] IEC 62471, Photobiological safety of lamps and lamp systems, International Electrotechnical Commission, Geneva, 2006.

[17] IEC 60825-1, Safety of laser products — Part 1: Equipment classification and requirements, 3rd ed., International Electrotechnical Commission, Geneva, 2014.

[18] CISPR 11, Industrial, scientific and medical equipment — Radio-frequency disturbance characteristics — Limits and methods of measurement, International Electrotechnical Commission, Geneva, 2015.

[19] EN 12464-1, Light and lighting — Lighting of work places — Part 1: Indoor work places, European Committee for Standardization, Brussels, 2021.

[20] ECRI, "Top 10 health technology hazards," ECRI Institute, Plymouth Meeting, PA, annual report series.